

Aggregation in the Marine Environment

GEORGE A. JACKSON* AND ADRIAN B. BURD

Department of Oceanography, Texas A&M University,
College Station, Texas 77843

The spatial distribution of chemical elements in the ocean is controlled by particles (including organisms); aggregation controls the particle properties. Coagulation is an important mechanism for controlling the size of marine particles and thereby their transport properties. Coagulation theory has provided a framework for the calculation of aggregation rates and size distributions. The use of fractal scaling to relate aggregate length to mass has been an important development that still needs to be fully incorporated into mathematical expressions for particle collision rates. In addition, disaggregation has emerged as an important process that is poorly described mathematically. Observations of particle spectra in the ocean are in general agreement with those expected for coagulation processes but tend to be for too small a size range to include the effects of particle disaggregation. Analysis of material caught in sediment traps suggests that aggregates are the dominant form of material falling through the ocean. An important aspect of the marine system is the presence of multiple particle sources that can confound fractal scaling based on single source particles. Coupled coagulation and chemical reaction models have become important tools in the interpretation of Th distributions. Further development of coagulation theory to describe marine systems promises to push the limits of our understanding of coagulation processes and their implications.

Introduction

Particulate material is an important component of the marine system. This material ranges from submicron-sized colloids to whales and possibly larger organisms (1). Biological and chemical processes transform dissolved material into particles and back to dissolved matter. Smaller particles are suspended in the water column and help control the chemistry of oceanic waters; larger particles (Figure 1) settle through the water column controlling the vertical distribution and transport of material. These two particle classes are not independent but are connected through aggregation and coagulation of the suspended particles into the larger settling particles. Coagulation produces larger particles by the repeated collision and joining of smaller ones. Dissolved and colloidal material can also participate in this transformation to large aggregates by adsorption onto or reaction with particles and subsequent coagulation. Because size is important in determining transport properties, aggregation of small particles into larger ones profoundly affects the fate of material in aquatic environments. Biological organisms also aggregate and disaggregate organic matter by feeding-

,metabolizing, rejecting as feces, or other processing of it as well as producing new particles from dissolved materials as they grow and divide. We will use the term coagulation to distinguish aggregation via physical processes from that resulting from biological processes.

The present review will concentrate on coagulation in marine systems, particularly its role in removing organic matter from the near-surface zones and its interaction with biological systems. Understanding the role of coagulation in such systems is complicated by the existence of those biological processes that alter particulate carbon concentrations and fluxes and that traditionally have been seen as the factors controlling the fate of organic matter in the ocean. As a result of the emphasis on organic matter, this review does not address work in the predominantly inorganic realm of the benthic boundary layer (e.g., refs 2 and 3) or of estuaries (4, 5). Despite the emphasis on the ocean, this work owes a debt to the work on freshwater systems that has been an inspiration to studying the mechanisms and affects of coagulation of biological particles (organisms) (e.g., refs 6 and 7). In our emphasis on observations as well as theory, this review differs from previous ones that have emphasized modeling of the processes (8, 9).

Particles differ from dissolved substances by the increased importance of physical processes in determining their fates and effects. On a small scale, chemical reactions within particles can be constrained by rates of reactant transport from solution. In conjunction with the vertical orientation provided by gravity, particles redistribute material in the water column. In their vertical movement and resulting increased concentration gradients, they differ from dissolved materials for which mixing should smooth concentration differences through time.

Aggregation changes particle properties and, thereby, their interactions with the marine environment. By combining small, slowly settling particles into larger faster settling ones, aggregation can enhance particle removal from surface waters. For example, aggregates in the 2.4–75 mm size range settle at an average of 25 times more rapidly than single algal cells (10–12). Coagulation can affect planktonic distributions and ecological interactions by selectively removing some algal species because of their size, shape, or surface properties; it can alter zooplankton feeding by removing food and by combining small particles too small to eat into larger packages that can be consumed; it can increase the removal rate of surface active chemical elements from oceanic surface waters.

Size Spectra and Coagulation Theory. The importance of size and number in determining particle interactions requires measures describing the relationship between particle size and concentration. One frequently used measure is the cumulative particle concentration $N(d)$, i.e., the number concentration of particles having an equivalent spherical diameter greater than d . The cumulative particle distribution can also be represented in terms of other

* Corresponding author voice: (409)845-0405; fax: (409)847-8879; e-mail: gjackson@tamu.edu.

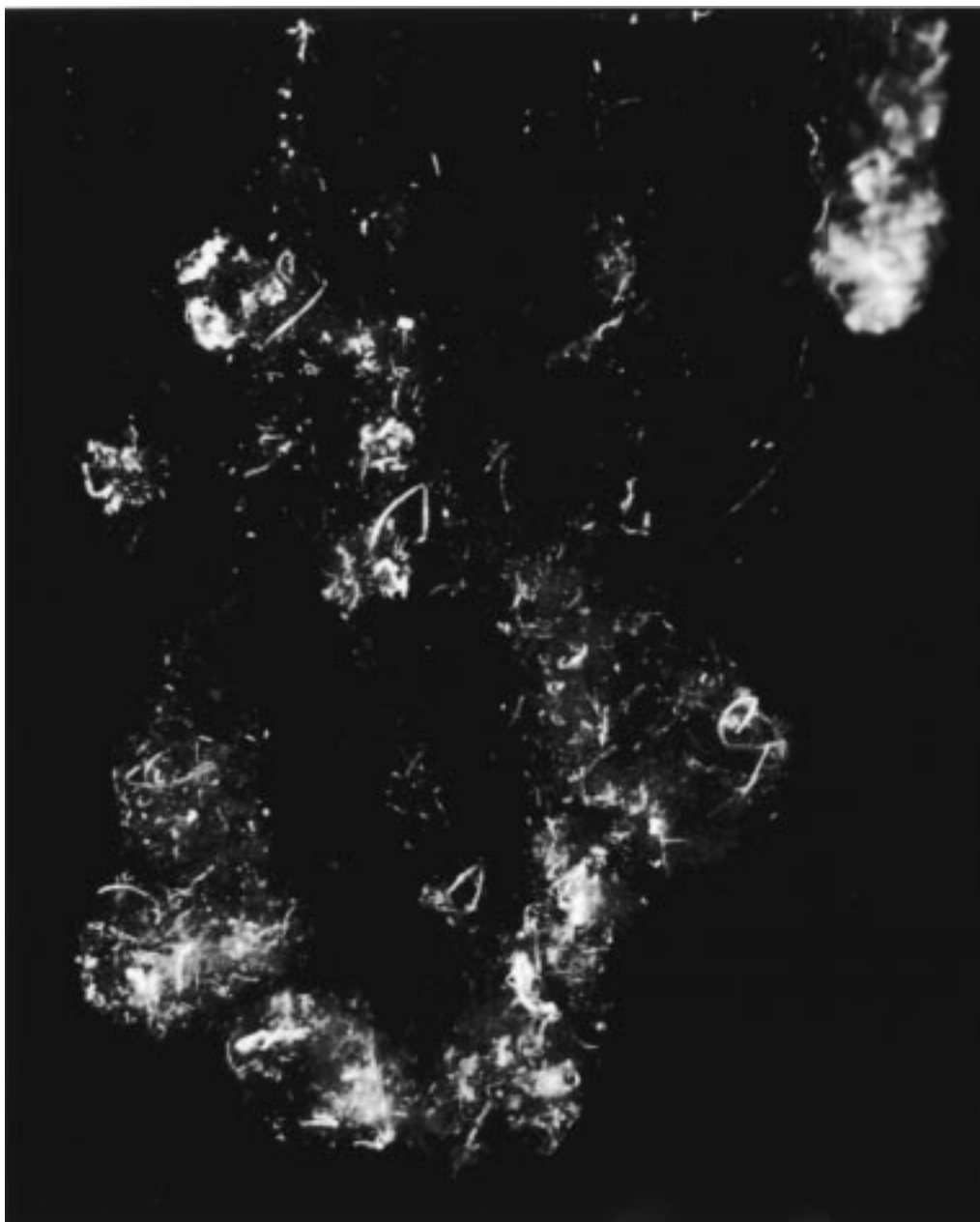


FIGURE 1. Picture of marine snow aggregate taken in situ, courtesy of A. L. Alldredge. The aggregate is about 1 cm across. It is composed primarily of marine diatoms, although fecal pellets can also be seen on it. The aggregate is held together with transparent material, presumably TEP. Several smaller aggregates can be identified as part of it, as can extensive void regions. Reprinted from cover photograph of *Deep-Sea Res. II*, Vol. 42, No. 1, 1995, with permission from Elsevier Science.

measures of particle size, including particle mass m . The differential particle size spectrum $n(d)$, frequently known simply as the particle size spectrum, is a convenient means to represent particle distributions as a density function. The size spectrum is effectively the number concentration per unit particle size interval and is related to $N(d)$ by

$$n(d) = -\frac{dN(d)}{dd} \quad (1)$$

It is relatively simple to transform between spectra based on different measures of particle size by using the chain rule if one knows the relationship between the measures being used. For example, the relationship between spectra expressed in terms of conserved volume ($v = (\pi/6)d^3$) and d is given by

$$n(v) = n(d) \frac{dd}{dv} = n(d) \frac{2}{\pi} d^{-2} \quad (2)$$

The particle number size spectrum is a useful function for calculating other properties of a system such as the volume spectra (i.e., the distribution of particle volume concentration with size) that can be used to calculate the total particulate volume. When dealing with coagulation theory, it is convenient to express the particle size spectrum in terms of particle mass as this is conserved in particle collisions. Using the above transformations, particle size spectra from a diverse group of instruments have been combined into a single spectrum covering a wider range of particles (13). Such transformations require that there be one dominant source particle for the fractal scaling to be valid.

Coagulation theory describes changes in the particle size distribution resulting from particle collisions involving all relevant particle size classes. The rate at which two particles

having masses m_i and m_j and concentrations C_i and C_j collide is given by the expression $[C(m_i)C(m_j)\beta(m_i, m_j)]$ where $\beta(m_i, m_j)$ is referred to as the coagulation kernel. Once a collision has occurred, the particles may stick together to form a new particle. The resulting formation rate for two particles of mass $(m_i + m_j)$ is $[\alpha C(m_i)C(m_j)\beta(m_i, m_j)]$ where α is the sticking probability, a measure of the probability that the two particles will adhere once they have collided.

Concentration changes for any given particle size class depend on all the collisions that can either add or remove particles from that size class. Particles are added by the collision and sticking of any two particles, the sum of whose masses lies within that of the desired size class; particles are subtracted when one of the particles in the size class collides with a particle whose size is large enough for the resulting new particle to have a mass greater than any in the size class. For a continuous range of particle sizes, the resulting rate of change of the particle spectrum can be given by an integro-differential equation (14, 15):

$$\frac{dn(m)}{dt} = \frac{\alpha}{2} \int_0^m \beta(m_j, m - m_j) n(m_j) n(m - m_j) dm_j - \alpha n(m) \int_0^\infty \beta(m, m_j) n(m_j) dm_j \quad (3)$$

where the particle size spectrum, $n(m)$, is now given in terms of particle mass. The first term is the rate at which collisions form new particles with masses lying between m and $m + dm$; the second term is the rate at which particles are lost from the same mass interval by coagulation.

Classic coagulation theory emphasizes three basic mechanisms for particle-particle contact: Brownian diffusion, laminar and turbulent shear, and differential sedimentation. The coagulation kernels for each are denoted by $\beta_{Br}(m_1, m_2)$, $\beta_{sh}(m_1, m_2)$, and $\beta_{ds}(m_1, m_2)$, respectively, and are functions of system physical properties as well as the sizes of the interacting particles. The total coagulation kernel is usually calculated as the sum of coagulation kernels for the three processes: $\beta = \beta_{Br} + \beta_{sh} + \beta_{ds}$. Formulations for the coagulation kernel can be quite complex (e.g., ref 16) and will not be presented in detail here.

Calculation of β_{ds} and β_{sh} involves analyzing the interaction of the colliding particles with the surrounding fluid. Early calculations imbedded the particles in background flows (rectilinear models), ignoring the effects of the particles on the fluid and, secondarily, each other (e.g., refs 17 and 18). More recent calculations have included detailed descriptions of the effect of the particles on the flow fields (curvilinear models) (e.g., ref 16); the curvilinear kernels predict much smaller collision rates between particles of dissimilar sizes. Calculations of collision rates between two impermeable spheres have been refined further by including the effects of van der Waals forces between the particles (e.g., ref 19). Observed density-size relationships have also been incorporated into calculations for differential sedimentation (20, 21). These more detailed calculations are typically performed only for the simple geometry of a solid sphere, making the application of these results to irregular, porous aggregates problematic.

Two important parameters for determining the coagulation rate of a particle are its mass and length. Early coagulation models assumed that particle volume is conserved when two particles collide, implicitly assuming that all particles are spherical and have constant density and porosity. However, aggregates formed by coagulation have a porosity that increases with aggregate size (e.g., ref 22), a relationship that has been observed in marine aggregates (e.g., ref 23). Aggregates formed from a single type of source particles (monodisperse systems) can be described using a fractal scaling relationship such that the mass, M , and size,

L , of an aggregate are related by

$$M \sim L^D \quad (4)$$

where D is the fractal dimension of the aggregate. For aggregates that conserve volume upon collision, $D = 3$; values of $D < 3$ indicate that the particle density decreases as particle mass increases.

Fractal dimensions have been calculated for marine aggregates using a variety of approaches yielding values of D in the range of 1.3–2.3 (e.g., refs 13 and 23–26). Part of this variability can be ascribed to the different techniques used to measure the particle sizes in different size ranges. While these values represent a wide range, it is significant that they are all less than 3.

Not all marine aggregates are fractal. Chin et al. (27) have formed aggregates by passing bubbles through seawater containing dissolved organic matter. These aggregates exhibited a gel structure that should be characterized by a different scaling with size than that of fractals because of the “annealing” that combines them.

Theoretical calculations of particle collision rates have dealt almost exclusively with spherical particles. The variable porosity of real aggregates can alter these theoretical estimates. For example, water flowing through a porous aggregate can lead to increased contact rates with small particles relative to those for an impermeable sphere. This can result in estimates of the collision rates that lie between those given by formulas that neglect (rectilinear) or incorporate (curvilinear) the fluid flow around a solid sphere. Calculations based on spherical particles with a constant porosity suggest that the capture of small particles within larger aggregates can be an important contribution to the particle collision rate (28). Relaxing the condition of constant porosity, using instead a radially varying porosity obeying a fractal scaling law, shows that the collection efficiency of an aggregate decreases with increasing fractal dimension (29). This trend has been observed in experimental measurements of the interaction between large aggregates and small beads (30, 31). These experiments also measure collision rates that lie between those given by formulas that neglect (rectilinear) or incorporate (curvilinear) the fluid flow around a solid sphere.

The effects of the fractal structure of an aggregate on the fluid flow around it are often embodied in the “hydrodynamic radius”. The hydrodynamic radius of an aggregate is the radius of an impermeable sphere having the same far field hydrodynamics as the aggregate (32). Numerical simulations of the drag on a fractal aggregate show that the hydrodynamic radius is proportional to the radius of gyration of the aggregate, with the proportionality constant being approximately 1 (32, 33). Experimental measurements of aggregate settling velocities indicate that the numerical simulations overestimate the drag on the settling aggregate (34).

Unfortunately, the fractal relationship is limited to systems where all the solid source particles are the same size (monodisperse systems). Natural systems are heterodisperse, with multiple particle sources—including organic colloids, clays, bacterial and algal cells, fecal pellets, animal molts and feeding structures—making it difficult to apply fractal scaling to describe the relationship between mass and length. The properties of aggregates formed in such systems can be described by a new extension to fractal scaling that expresses fractal scaling as a geometric property. Using this, Jackson (35) derived a quantity related to length ($\lambda = L^p$, where L is the particle length) that is conserved in the same way as mass is conserved during coagulation. Using mass m and this new length parameter to describe a two-dimensional particle size spectrum $n(m, \lambda, t)$ allows the coagulation equa-

tions to be solved in ways that distinguish large TEP (transparent exopolymeric particle—see below) aggregates from fecal pellets of the same mass and that treat the aggregates that they form in different ways.

The opposing process to aggregation is disaggregation, by which large particles are broken up into smaller ones. Disaggregation can arise as a result of either physical or biological processes or a combination of the two. Physical disaggregation occurs when the motion of water relative to the particle gives rise to frictional forces or pressure differences that are sufficient to break the particle apart. Several possibilities arise: the particle can fragment into a number of particles having a range of sizes (e.g., ref 36); the particle can fragment into two equally sized daughter particles (e.g., ref 37); single small particles can be eroded from the surface of the larger particle (e.g., ref 38). Theories and models of disaggregation are more stochastic in nature than corresponding aggregation theories for several reasons. Foremost is that it is impossible to predict the number and size distribution of daughter particles arising from the disaggregation of a single large particle. As a result, some assumptions must be made concerning the probabilities of forming daughter particles of certain sizes (39, 40). Pandya and Spielman (39) combined the fragmentation and erosion scenarios into a single formalism, using probabilities for each. They chose a normal distribution to determine the size distribution of daughter particles in the case of splitting, and the probability of producing erosion products of a certain size was given by a log-normal distribution. While this does incorporate the dominant possibilities, it does require extensive experimental input and may be more complicated than necessary.

Disaggregation is not often incorporated into models of marine particle size spectra because of the difficulty of incorporating the kinetics of disaggregation into the aggregation models and from the lack of data that would allow such models to be formulated and verified. Hill and Nowell (3) and Jackson (41) applied models of different levels of complexity to the problem. Jackson showed that in order for an aggregation model to successfully predict the particle size spectrum measured in a mesocosm, disaggregation had to be included in the model. Hill and Nowell (3) and Hill (40) incorporated the detailed stochastic model of Pandya and Spielman (39) into models for sediments in bottom boundary layers and suspended flocs. Pandya and Spielman (39) originally proposed that the frequency of floc erosion was proportional to the fluid shear rate. This would imply that for a given shear rate all particles, irrespective of their size, would experience the same erosion rate. As pointed out by Hill (40), this is probably unrealistic for flocs in turbulent flow since particles smaller than the smallest eddy size would not experience great shear forces. Hill proposed a floc erosion rate that depended upon the particle size. Results from the model indicate that splitting of flocs rather than erosion is the dominant disaggregation process and that particles smaller than about 100 μm did not suffer appreciable breakup.

Including disaggregation in these models requires the specification of a series of coefficients whose values are poorly known. Among these is the strength of the particle bonds holding the floc together (e.g., ref 42). Jackson (43) used a simpler model that incorporated results from the measured breakup rates of clay flocs (44) to demonstrate a linear relationship between the logarithm of the disaggregation rate and the logarithm of the particle diameter, allowing a simplified description of disaggregation into a coagulation model.

Particle disaggregation can also occur through biological interactions. Bacteria and zooplankton can feed on the aggregate and remineralize the material or sufficiently weaken

the structure of the aggregate that it breaks apart at shears lower than those without their intervention (45, 46).

Observations of Particles Distributions and Fluxes

The sizes of marine particles vary from the colloidal (1 nm – 1 μm) to marine snow (~1 cm). Most measurements of particle size distributions have been made for material larger than 1 μm and are usually made over small ranges of particle size because the instruments being used have resolutions peaked in particular size ranges. For example, resistance counters such as the Coulter and Elzone counters are typically used for particles having diameters in the range of 3–50 μm ; photographic techniques typically are used to measure particles having diameters in the range of 50–1000 μm . Measuring particle properties of the environment presents a range of problems. Because particle distributions are determined by the dynamic interaction of multiple processes that do not all stop when a sample is collected and isolated from the environment, particle properties change while samples wait to be analyzed (47). For example, bacterial growth can degrade organic material, and coagulation can change particle distributions (48). Adding preservatives at concentrations high enough to suppress bacterial activity can produce artifacts by precipitating new particles or changing particle surface activity (48).

Processing the samples can introduce its own set of artifacts. For example, the accumulation of particles at the sample/filter interface can cause enhanced particle coagulation and thereby removal of particles that should be small enough to pass through a filter (48, 49). The commonly used aperture-impedance particle counter (e.g., Coulter counter) can tear apart particles while they pass through the small orifice and alter the reported particle size (2, 50). Other particle measurement techniques can be equally disruptive (2, 48) and affect reported particle properties.

Calibrating instruments is a major problem because of the difficulty of generating well-characterized particles with properties similar to those of environmental particles. Optical and aperture-impedance particle counters are typically calibrated with solid, solitary spheres, such as polystyrene latex beads. The response of the instruments to aggregated, fractal, particles can differ from that of the solitary particles in ways that depend of the physics of the measurement (e.g., ref 13). For instruments that estimate bulk sample properties, the range of particle sizes and types in natural waters further complicate the interpretation of measurements. For example, measurements of fractal dimension for particles in a water sample using light scattering produces a result interpreted as that of the “average” particle but which is not rigorously defined (48).

The distribution of particle sizes in the marine environment often shows a power law behavior over commonly observed size ranges (e.g., ref 51):

$$N(d) = Ad^{-(\delta-1)} \quad (5)$$

where A and δ are constants (Figure 2). For $\delta > 1$, this states that there are far more small particles than large.

Colloidal particles have been detected with abundances exceeding 10^9 mL^{-1} (52–56). Particle concentrations increase nearly logarithmically with decreasing size (55). Size distributions of these nanometer-sized particles have been measured in the North Atlantic and Southern Oceans (56). Many of these spectra show a flattening of the spectrum at around 100 nm.

Sheldon et al. (57, 58) used Coulter counters to observe particle size spectra in the 1–100 μm size range. They found considerable variation in the spectra both with depth and geography, observing two types of depth variation. In subtropical areas, spectra taken at depth showed, as in surface

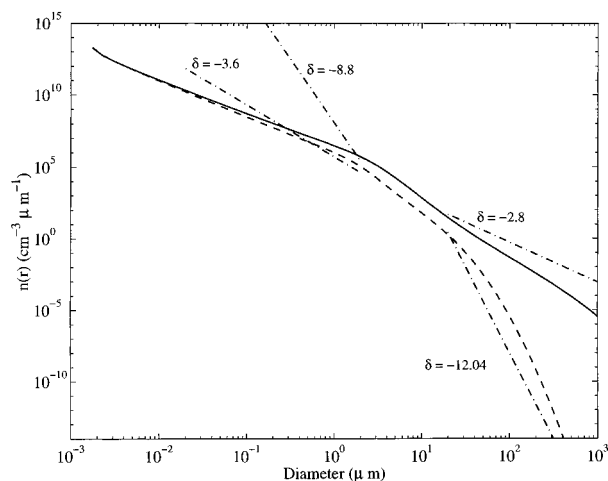


FIGURE 2. Modeled steady-state particle size spectra (solid and dashed lines) compared with measured slopes of particle size spectra (dash-dot line). The model spectra were calculated using a rectilinear coagulation kernel for particles with a fractal dimension of 2.6, a monomer size of 1 nm, a stickiness of $\alpha = 1$ and did not include disaggregation. The solid line shows a size spectrum with a shear of 0.1 s^{-1} and the dashed line with a shear of 1.0 s^{-1} . The dash-dot lines represent the range of slopes for the size spectrum that have been measured. For particles with diameter less than $1 \mu\text{m}$, the observed slopes are taken from ref 56. For the larger particles, observed slopes are taken from ref 64. The slope of the modeled size distribution for submicron sized particles lies below the observed range. Including disaggregation may increase this slope so that it agrees more with the observed slopes.

waters, roughly equal amounts of material in each size grade but with amounts that were less than spectra taken at the surface. In other areas, the spectra taken at depth were quite dissimilar from those near the surface. Deep waters tended to show more constant size distributions, although the total particle concentration was variable. They made the general observation that there are approximately equal amounts of mass (or volume) in size ranges whose maximum particle mass (or volume) is twice that of its minimum size range. These size ranges they called octaves.

Lal and Lerman (59) compared particle size spectra of foraminifera and diatoms both in the water column and in the underlying sediments. The size spectra for the material in the water column was steeper than the corresponding slope for particles in the sediments. To explain this observation, they considered models of particles that dissolved or fragmented. The former case resulted in a spectrum with a broad maximum near $3\text{--}5 \mu\text{m}$; the latter led to a spectrum for the residual particles that had a steeper slope than the parent particle distribution. Lerman et al. (60) examined particle size distributions in the North Atlantic and calculated values of $\delta = 0.44$ and 5.13 for particles with $2 < d < 16 \mu\text{m}$.

In a paper collecting various size spectra, McCave (61) found that below $200\text{--}400 \text{ m}$, particle sizes follow a power law distribution with δ lying between 3.4 and 4.6 . He concluded that aggregation of particles is the norm and that although a slope of 4 is usually assumed, there is considerable variation in this value (as was confirmed by later observations). In a thoughtful and insightful paper, McCave (62) explored the role of coagulation in greater detail, concluding that it dominated the nepheloid layer near the ocean bottom because of the high particle concentrations there. He also argued that aggregation is slow in the mid-depth regions of the ocean because of the low particle concentrations there.

Bishop et al. (63) examined the size distribution of foraminifera fragments and fecal material in the South

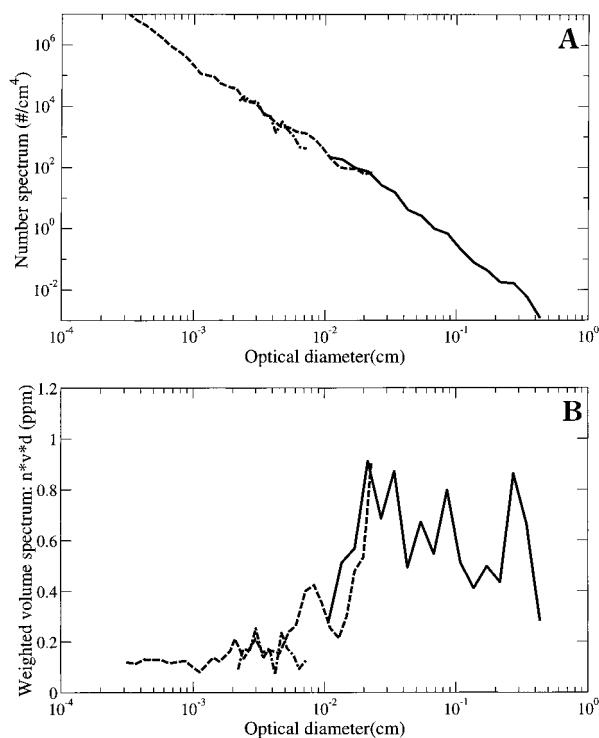


FIGURE 3. Particle size spectrum assembled from measurements by multiple instruments for water at 10 m in Monterey Bay, CA, July 29, 1993 (7). Solid line: in situ optical instrument; dashed line: Coulter counter; dash-dot line: image analysis system of filtered sample. A: number spectrum; B: weighted volume spectrum for the conserved volume, equivalent to particle mass. The weighting makes the area under any part of the curve proportional to the total volume for that part.

Atlantic using particles collected on a series of filters as part of an in situ filtration system. All the size distributions were measured for particles larger than $53 \mu\text{m}$ and were taken from the top 400 m of the water column. The size distributions for foraminifera ranged between $\delta = 5.1$ and $\delta = 8.7$; the size distribution for fecal material had slopes ranging between 3.8 and 5.9 . This represents a wider range than seen by McCave (61) and, in the case of the foraminifera, does not support the earlier observation of equal particulate volume in equal size intervals (57). A greater range of slopes was found for waters in the east Pacific (64). In this case, the particle size distributions for particles larger than $53 \mu\text{m}$ were measured at 12 depths between 15 and 1500 m . Slopes for the size distribution of foraminifera ranged between 5.37 and 12.04 , whereas for fecal material, δ had values lying between 2.8 and 5.6 . There was no clear trend of spectral slope with depth.

Jackson et al. (13) combined measurements from different instruments to yield spectra from about $1 \mu\text{m}$ to 1 cm (Figure 3). By using fractal scaling on particle diameters, they converted between diameters determined with Coulter counters and image analysis systems. The values of δ depended on which diameter was being used, being $2.96\text{--}3.00$ for the image diameter and $3.50\text{--}3.61$ for the Coulter counter. More informative was the display of mass distribution, which showed that most of the particle mass was in the greater than $100 \mu\text{m}$ size fraction.

Particle number concentration in marine systems is dominated by the smaller particles, whereas the flux of material through the water column is dominated by relatively rare, large particles (e.g., refs 61–64). The large range of observed size distribution slopes indicates that several processes are operating and makes predicting size distribu-

tions more of a challenge.

Observations of Particle Composition and Fluxes in the Oceans

The most basic evidence of particle aggregation in the marine environment is from direct observation of aggregate occurrence. Large aggregates, also known as marine snow, have been observed and studied by divers in surface waters (e.g., refs 65–67). These large aggregates can include diatoms, bacteria, protozoa, fecal pellets, discarded zooplankton feeding structures, and amorphous organic detritus. Such flocs can form after diatom blooms (10, 11). Aggregates have also been observed as they sink in the water column, increasing their average size with increasing depth (68). Both sediment trap data and in situ camera observations indicate that marine particles do indeed settle as aggregates (69–71).

One of the most important properties of particles is that large particles tend to fall faster than smaller ones. Differences in the timing between peaks in the surface particle concentration and peaks detected by sediment traps deployed throughout the water column indicate that the dominant particles have settling rates of 50–100 m d⁻¹ or more (72, 73). These rates are far faster than those for a single cell (roughly 0.1 m d⁻¹), implying that the particles are settling as aggregates. This has been observed for algal cells (12), for marine snow particles (10, 11, 69), and for theoretically calculated aggregate settling rates (32). Logan and Wilkinson (23) used the observed relationship between sinking rate and particle size to infer a fractal dimension. Lampitt et al. (74) observed a diel variation in particle concentration and flux at 270 m whose timing varied with particle size. Ruiz (75) argued that disaggregation associated with diel cycles of turbulence was the most reasonable explanation for the timing of Lampitt's observations. Graham (76) argued that this was the result of diel cycles in zooplankton feeding and the resulting destruction of mixed layer aggregates.

Aggregation of particles in the surface waters has consequences for the deeper oceanic regions. There is extensive evidence implying that aggregates represent the dominant agents of organic matter sedimentation. Large aggregates have been observed using camera systems in the water column and their concentrations correlated with material collection rates in sediment traps (77). Examination of the contents of sediment traps has shown that fecal pellets constitute a relatively small fraction (10–30%) of the C flux (70, 78, 79). Thus, the dominant source of sedimenting material is nonfecal pellet particles, presumably mostly aggregates.

Newton et al. (80) examined the vertical flux and composition of sinking material at the JGOFS North Atlantic Bloom Experiment (NABE) study site, finding that particle export tended to occur in pulses, or events, and that the composition of the material varied with time and event. Particles associated with some events were high in mucopolysaccharides while others were not. The high mucopolysaccharide concentrations provide support for the idea that TEP can be important in aggregate formation and carbon export (see below). The C:N values of the material varied through time and, presumably, reflected the changing composition of aggregates.

The effects of aggregation at the ocean surface affect biological processes on the ocean floor. Rapidly accumulating algal mats have been observed on the floor of the North Atlantic after a surface algal bloom (81–83). On the floor of the North Atlantic, at depths between 1370 and 4000 m, Billet et al. (81) observed the appearance of large concentrations of algal cells soon after the spring bloom in overlying waters. Comparisons of the timing of these arrivals with the spring bloom again led to the conclusion that the material was falling

at speeds of between 100 and 150 m d⁻¹. Such rates are inconsistent with the known fall velocities of single cells (12) but are consistent with those of aggregates (10).

TEP. Transparent exopolymer particles (TEP) have recently been observed in marine waters (84). These particles can be observed on filters only after staining with alcian blue. They vary in diameter from <2 to >100 μm and can be abundant (>5000 mL⁻¹) in the marine environment (84–86). The high mucopolysaccharide concentrations in sedimenting material during some sedimentation events observed by Newton et al. (80) support reports that TEP may be important in the aggregation process.

Several hypotheses exist for the formation of TEP. One such model is that TEP form abiotically via the coagulation of colloidal organic material (86–92). TEP also appear to be formed as a result of excretion of organic matter by algae (90). Mopper et al. (89) found a correlation between concentrations of surface carbohydrates and TEP, arguing that both were continually produced by algal exudation.

TEP can be an important ingredient in the process of aggregation. In many circumstances, traditional particle concentration alone does not explain aggregate production. The presence of TEP at sufficient concentrations has been proposed as a crucial factor in the formation of aggregates (85, 90, 91), although other observations have not found it to be the crucial factor (93). There are at least two mechanisms by which TEP could influence coagulation: by increasing particle numbers and by changing the stickiness of the algae (41). Experimental evidence suggests that both occur (92, 94). Logan et al. (91) compared residence times of TEP and phytoplankton in different systems, concluding that while TEP may not be needed to explain all diatom blooms, TEP do regulate the formation of diatom blooms in marine surface waters. Observations are consistent with aggregation models involving only cell–cell interactions that do not involve TEP (94). This is an area of ongoing research.

Modeling Particle Size Distributions

Various approaches have been used to model the particle size distribution in marine waters. Platt and Denman (95, 96) used what were essentially dimensional arguments relating organism turnover time as a function of biomass and organism respiration to predict a particle size spectrum that was controlled by organism interactions. The result was a particle size spectrum similar to that of Sheldon et al. (57, 58). They did not explain the role of nonliving detrital matter nor provide a detailed mechanism of the interactions responsible. It is, thus, particularly interesting that Rodriguez and Mullin (97) observed reasonably similar size spectra when they sorted zooplankton caught in nets into size categories and measured the biomass of each organism.

The observed power law size distributions found in marine systems led Hunt (17) to apply the techniques used for modeling aerosol size distributions pioneered by Friedlander (12). The derivation of a self-similar spectrum required the assumptions that only one coagulation or sedimentation mechanism dominates in any particular particle size range and that the particle size distribution is in a steady state. With these assumptions, Hunt showed that particle size spectra in the ocean would be expected to have the following exponents: $\delta = 2.5$ for Brownian coagulation, 4 for shear coagulation, 4.5 for differential sedimentation, and 4.75 for settling. Brownian coagulation should dominate for particles with diameter less than 2 μm, shear between 2 and 40 μm, and differential sedimentation and settling for diameters greater than 40 μm. Hunt was able to show good agreement with observational spectra.

Hunt's calculations did not include the fractal nature of the marine aggregates. Jiang and Logan (98) extended Hunt's work in such a way that the fractal dimension of the aggregates

could be inferred from the observed slope of the particle size spectrum. From this they inferred that aggregates forming by shear coagulation had fractal dimensions of 2.4, whereas those forming from differential sedimentation had fractal dimensions in the range of 1.6–2.3.

Comparison of the self-similar particle size spectrum with a steady-state spectrum calculated numerically shows that the assumptions underlying the self-similar spectrum are not always valid (17, 99). Agreement between the spectral slope of the self-similar distribution (98) and the numerical simulation occurs only for the size range dominated by Brownian coagulation. In order for the numerical model to fit the slopes predicted by the self-similar model for the whole size range, there had to be no settling in the numerical model and only one coagulation mechanism was allowed to operate in each size interval.

The particle size spectra in simple particle systems often converge on similar shapes. Farley and Morel (100) took advantage of this to determine power series relationships between sedimentation rate and particle concentration for a system with a pulsed colloid input. Burd and Jackson (101) have updated the work of Farley and Morel to include both fractal scaling for aggregates and more recent formulas for particle collision rates. Such simple formulas allow estimates of coagulation effects to be made without having to solve the entire set of coagulation equations.

The coagulation equation can be solved analytically only in very special cases. For more general situations the equation must be solved numerically, and various approaches have been developed to do this (for a comparison of different methods, see ref 102). The sectional approach (103) divides the total particle mass range into intervals (sections), frequently with upper limits twice that of their lower limits. In this approach the particle size spectrum is treated as a series of histograms (103). Because the spectral shape is assumed constant within a section, only the total particle mass is allowed to vary. This allows the coagulation integro-differential equation (eq 3) to be transformed into a series of coupled ordinary differential equations that can be solved numerically using standard techniques (e.g., refs 43 and 104). This approach can still involve the solution of a substantial number of equations. For example, it required 52 sections and as many simultaneous ordinary differential equations to consider the interaction of particles ranging from colloids to marine snow (101).

Uses of Coagulation Models

Aggregation helps control the size distribution of particles in the marine environment. As a consequence of this, it is a factor in determining the flux of material from the ocean surface to the ocean depths. Additionally, coagulation can help in understanding the demise of algal blooms, the scavenging of trace metals, and the formation of TEP.

Coagulation theory has been used to explain particle removal in different regions of the ocean. Particles, including submicron colloids, are removed from riverine waters as the salinity increase associated with the mixing with marine waters destabilizes the small suspended particles and allows them to coagulate and settle (e.g., refs 105–107). Coagulation of particles suspended in the bottom boundary layer enhances their settling to the ocean floor (3, 62, 108, 109).

Coagulation and Algal Dynamics. Simple models of particle dynamics in marine systems have small particles colliding and sticking to form ever larger, more rapidly falling particles that ultimately sink out of the system. With continual introduction of new particles by mechanisms such as algal growth or colloid formation, the system achieves a mass distribution that is relatively evenly distributed in logarithmic particle size intervals (1, 57).

A simple model of algal growth, coagulation, and subsequent loss to sedimentation has shown that coagulation can place an upper limit on algal concentrations despite continued algal divisions (109). An index gives the maximum concentration as a function of mixed layer depth, particle settling velocity, algal diameter, shear, and particle stickiness. [The formula in ref 109 is off by a factor of 2 because of an error in calculating the removal rate from collisions of identical particles: $1 + \delta_{ij}$ should be 1. The corrected formula for the critical concentration is $C_{cr} = 0.024\mu(\alpha\gamma)^{-1}r^{-3}$, where μ is the modified specific growth rate, γ is the shear rate, α is the particle stickiness, and r is the radius of a single alga.] It was remarkably successful in predicting maximum bloom concentrations in the North Sea (8, 110) and, when appropriately modified to account for multiple diatom species, in a Danish fjord (94).

Aggregation rates can be affected by properties of the algal cells, such as the presence of spines, the tendency of some algal species to form chains, and variations in the stickiness of the cells (8). Laboratory studies with algal cultures have shown that algal cells do indeed have a finite chance of sticking when they collide, that this chance can change with the nutritional state of the algae, and that the effect of nutritional state depends on the algal species (111).

While the modeling results discussed here have emphasized algal–algal interactions, there are other classes of particle in the sea that can also participate in the coagulation process. Hill (112) has argued that these background particles may be necessary to initiate rapid coagulation. Whether or not this is the case, the interaction of aggregates composed predominantly of algae with other particles could enhance their removal as well. Such particles could include TEP, colloids, and other organisms.

Mari and Burd (113) presented a comparison of observed and modeled TEP size spectra. The data were collected in the Kattegat (Denmark) over the period of 1 year. The model involves TEP particles and particles regarded as aggregates (called non-TEP) containing TEP, algal cells, and detritus. The non-TEP particles were not actively modeled but were assumed to form a background having a constant particle size spectrum. This model reproduced the TEP particle size spectrum quite well (R^2 values varied from 0.77 to 0.99), although discrepancies occur for both large and small particles. At the smaller end, this may be due to biology or uncertainties in the shear or both. The models indicate that particle stickiness is important, in particular the stickiness between TEP and non-TEP particles.

Modeling of TEP introduces a fundamental problem, that of modeling the aggregation of a multicomponent system, because marine aggregates are a heterogeneous collection of diatoms, detritus, fecal pellets, discarded zooplankton feeding structures, and general detritus. However, it is hoped that on the average marine aggregates display some degree of homogeneity. If TEP forms the matrix in which the particles aggregate, then this picture would have to change.

Stoll and Buffle (114) have simulated that the interaction of organic and inorganic colloids to show that the dynamics of aggregate formation and the resulting fractal scaling depend on the nature of the organic molecules. In their system, which allowed sticking only when the contact was between an organic and an inorganic unit, coagulation rates were significantly slower than if all possible collisions stuck.

There has been recent appreciation of the role of disaggregation in controlling particle size distributions and, as a result, sedimentation rates. Jackson (43) modeled the development of particle spectra in a mesocosm studied by multiple investigators as part of SIGMA (Significant Interactions Generating Marine Aggregates—an Office of Naval Research funded program). He found it necessary to include disaggregation along with coagulation in order to explain

the experimental observations. One characteristic of both the observed and theoretical particle size spectra was that most of the mass was concentrated in a relatively small size range of larger particles (about 0.2 μm), despite the presence of a phytoplankton particle source. A similar mass distribution was observed in the waters of Monterey Bay (Figure 3), where there were large concentrations of marine snow particles observed (13), but not at East Sound in Washington (115), where there was no such evidence of aggregate formation.

Adsorption and Removal of Thorium. Aggregation plays a pivotal role in the scavenging of trace metals from surface waters in the ocean. Small particles, such as colloids, play a dominant role in the adsorption of surface reactive trace metals because of their large surface area-to-volume ratio. The trace metals can be subsequently removed from the surface waters if the smaller particles can aggregate into larger, rapidly settling particles. ^{234}Th ($t_{1/2} = 24.1$ days), a particle-reactive radionuclide produced in situ from soluble ^{238}U , has been used in JGOFS (Joint Global Ocean Flux Study) as a tracer to estimate upper ocean POC export (116–121). The role that aggregation plays in determining the export of thorium from the upper ocean is reflected in particle aggregation being incorporated in models used to interpret thorium profiles in the ocean (e.g., refs 122 and 123).

Estimating carbon export fluxes from thorium radioisotope measurements requires knowing the carbon-to-thorium ratio for the particles. This ratio can vary spatially, temporally, and with particle size depending upon biological productivity, particle export, and particle size distribution (118–120, 124). Observed decreases in the carbon-to-thorium ratio with increasing particle size have been attributed to preferential remineralization of particulate organic carbon via biological processes (117, 124). Burd et al. (125) have demonstrated that a purely physical–chemical model can reproduce this observed inverse dependence. Their model builds on the work of Honeyman and Santschi (122), combining a detailed particle aggregation model with a chemical adsorption model. Observations have shown that the carbon-to-thorium ratio can also increase with particle size (126, 127). The relative importance of physical, biological, and chemical processes in determining particulate thorium distributions is at yet unclear.

The behavior of the carbon-to-thorium ratio depends on the physics of aggregation forming particles of sufficient size to sink at appreciable rates, chemical adsorption determining the fractionation between dissolved and particulate phases, and biological interactions that can alter the chemical composition of particles through processes such as remineralization. All these processes depend on particle size. Most models used for interpreting thorium data make use of two, or at most three, particle size classes. Burd et al. (125) employed a sectional method using 52 size classes covering particle sizes ranging from the colloidal to marine snow. This approach allowed the dependence of coagulation and adsorption on particle size to be modeled in detail. A variety of adsorption models were examined, and some were shown to violate diffusion-limited constraints for certain particle size ranges (Figure 4). Comparison between the model and size fractionated field data are complicated by the latter being averages over the particle size spectrum. Similar averaging applied to the model results led to changes of up to 2 orders of magnitude in the colloidal carbon-to-thorium ratio.

Thorium measurements have also been used to obtain information on particle aggregation and recycling rates. As an example, Murnane et al. (127) used a simple two particle size-class model to fit ^{234}Th , POC and PON distributions, and sediment trap data from JGOFS North Atlantic Bloom Experiment (NABE) for a period of 5.5 weeks. Small particles

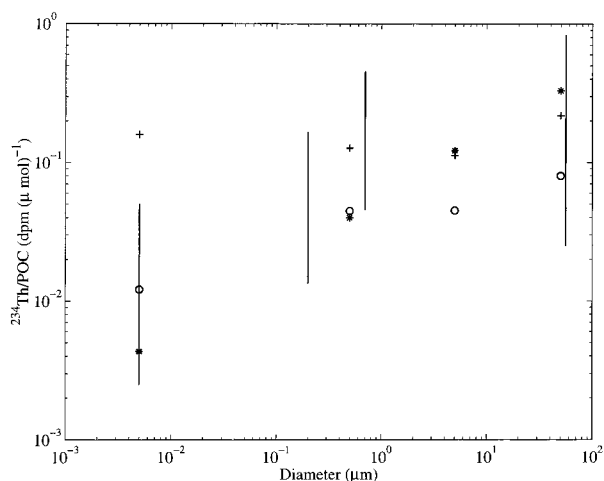


FIGURE 4. Ratio of ^{234}Th to particulate organic carbon as a function of particle diameter (125). The vertical bars represent the range of $^{234}\text{Th}/\text{POC}$ that have been observed (refs 116, 119, 124, 126, and 128 and Bruland, unpublished data). The results of three different simulations are shown using different symbols: (*) for a simulation in which the specific adsorption constant of ^{234}Th is assumed constant (123); (+) when the specific adsorption constant is transport limited; (C) for a combination of the two previous cases (see ref 125 for details). The model results are shown as the result of a simulated filter measurement made using the continuous size distribution predicted from the model.

became large, and vice versa, via aggregation and disaggregation, whose rates they described with terms that were linear in particle concentrations. Best fits were obtained with aggregation rate constants that varied by a factor of 38 (from 2 to 76 yr^{-1}) and disaggregation rate constants that varied by a factor of 3 (from 156 to 524 yr^{-1}) over little more than 1 month. The larger change in the aggregation rate is consistent with the fact that the aggregation “constant” should actually be proportional to particle concentration if the aggregation rate is to be proportional to particle concentration squared that coagulation theory predicts.

Future Directions

Particulate material controls the chemistry of the oceans as well as the vertical distribution of elements in the water column. All particles contribute, from the colloidal sized macromolecules to the large marine snow particles observed by divers. Understanding the interactions between particles and the manner in which small particles can get incorporated into larger, sinking particles is crucial for our understanding of the oceans. Aggregation has been used to help understand the dynamics of algal blooms and the transport of material from the ocean surface to the ocean deeps. It has also been used to understand the chemical kinetics of trace metal scavenging.

One outstanding challenge is incorporating the reality of multiple particle sources both in interpreting observations and in simulating system dynamics. This poses a particular problem for the fractal transformations that have become an important tool in interpreting data because of their implicit linkage to systems with single source particles. However, multiple particle types can affect the dynamics of aggregation, as with the interaction of organic and inorganic colloids (114). Furthermore, multiple particle sources do not accord with the assumptions made for such classical calculations as the self-preserving size spectrum.

Much remains to be done. It is now apparent that disaggregation must be incorporated into disaggregation models. Simple disaggregation models are already being used successfully. More sophisticated models are also being

used, but these require knowledge of parameters such as bond strengths which as yet are mostly unavailable.

Global biogeochemical models often do not incorporate aggregation when calculating vertical fluxes of material from the ocean surface to the ocean deeps. Relationships between quantities tracked in these models (e.g., chlorophyll) and fluxes can be developed using the aggregation models discussed in this review. These relationships can then be incorporated into the larger biogeochemical models. Steps along this path have already been taken with the work of Farley and Morel (100) and Burd and Jackson (101).

Acknowledgments

The authors would like to acknowledge the inspiration for this work provided by W. Stumm, C. R. O'Melia, and J. J. Morgan. A. L. Allredge provided the picture of an aggregate (Figure 1). This work supported by NSF Grant OCE-9726077.

Literature Cited

- (1) Sheldon, R. W.; Kerr, S. R. *Limnol. Oceanogr.* **1972**, *17*, 796–798.
- (2) McCave, I. N. *J. Geophys. Res.* **1983**, *88*, 7647–7666.
- (3) Hill, P. S.; Nowell, A. R. M. *J. Geophys. Res.* **1995**, *100*, 22,749–22,763.
- (4) Eisma, D. *Neth. J. Sea Res.* **1986**, *20*, 183–199.
- (5) Edzwald, J. K.; Upchurch, J. B.; O'Melia, C. R. *Environ. Sci. Technol.* **1974**, *8*, 58–62.
- (6) O'Melia, C. R.; Bowman, K. S. *Schweiz. Z. Hydrol.* **1984**, *46*, 64–85.
- (7) Wielenmann, U.; O'Melia, C. R.; Stumm, W. *Limnol. Oceanogr.* **1989**, *34*, 1–18.
- (8) Jackson, G. A.; Lochmann, S. E. *Environmental Particles*, Vol. 2; Buffle, J., van Leeuwen, H. P., Eds.; Lewis Publishers: Chelsea, MI, 1993; pp 387–414.
- (9) Jackson, G. A. *Aquatic chemistry: principles and applications of interfacial and inter-species interactions in aquatic systems*; Huang, C. P., O'Melia, C. R., Morgan, J. J., Eds.; American Chemical Society: Washington, DC, 1995; pp 203–217.
- (10) Allredge, A. L.; Gotschalk, C. *Deep-Sea Res.* **1988**, *36*, 159–171.
- (11) Allredge, A. L.; Gotschalk, C. *Limnol. Oceanogr.* **1988**, *33*, 339–351.
- (12) Smayda, T. J. *Oceanogr. Mar. Biol. Annu. Rev.* **1970**, *8*, 353–414.
- (13) Jackson, G. A.; Maffione, R.; Costello, D. K.; Allredge, A. L.; Logan, B. E.; Dam, H. G. *Deep-Sea Res.* **1997**, *44*, 1739–1767.
- (14) Smoluchowski, M. V. *Phys. Z.* **1917**, *17*, 557–585.
- (15) Smoluchowski, M. V. *Z. Phys. Chem. Stoechiom. Verwandtschaftsl.* **1917**, *92*, 129–168.
- (16) Pruppacher, H. R.; Klett, J. D. *Microphysics of clouds and precipitation*; Riedel: Dordrecht, Holland, 1980.
- (17) Hunt, J. R. *Particulates in water*; Kavanaugh, M. C., Leckie, J. O., Eds.; American Chemical Society: Washington, DC, 1980; pp 243–257.
- (18) Friedlander, S. K. *Smoke, dust and haze*; Wiley: New York, 1977.
- (19) Han, M.; Lawler, D. F. *J. Am. Water Works Assoc.* **1992**, *84* (10), 79–91.
- (20) Stolzenbach, K. D. *Deep-Sea Res.* **1993**, *40*, 359–369.
- (21) Stolzenbach, K. D.; Elimelech, M. *Deep-Sea Res.* **1994**, *41*, 469–483.
- (22) Vicsek, T. *Fractal growth phenomena*, 2nd ed.; World Scientific: Singapore, 1992.
- (23) Logan, B. E.; Wilkinson, D. B. *Limnol. Oceanogr.* **1992**, *39*, 130–136.
- (24) Klips, J. R.; Logan, B. E.; Allredge, A. L. *Deep-Sea Res.* **1994**, *41*, 1159–1169.
- (25) Li, X.; Logan, B. E. *Deep-Sea Res. II* **1995**, *42*, 125–138.
- (26) Jackson, G. A.; Logan, B.; Allredge, A.; Dam, H. *Deep-Sea Res. II* **1995**, *42*, 139–158.
- (27) Chin, W.-C.; Orellana, M. V.; Verdugo, P. *Nature* **1998**, *391*, 568–572.
- (28) Stolzenbach, K. D. *Deep-Sea Res.* **1993**, *40*, 359–369.
- (29) Veerapaneni, S.; Wiesner, M. R. *J. Colloid Interface Sci.* **1996**, *177*, 45–57.
- (30) Li, X.; Logan, B. E. *Environ. Sci. Technol.* **1997**, *31*, 1229–1236.
- (31) Li, X.; Logan, B. E. *Environ. Sci. Technol.* **1997**, *31*, 1237–1242.
- (32) Rogak, S. N.; Flagan, R. C. *J. Colloid Interface Sci.* **1990**, *134*, 206–218.
- (33) Bossis, G.; Meunier, A.; Brady, J. F. *J. Chem. Phys.* **1991**, *94*, 5064–5070.
- (34) Johnson, C. P.; Li, X.; Logan, B. E. *Environ. Sci. Technol.* **1996**, *30*, 1911–1918.
- (35) Jackson, G. A. *J. Colloid Interface Sci.* **1998**, *202*, 20–29.
- (36) Srivastava, R. C. *J. Atmos. Sci.* **1971**, *28*, 410–415.
- (37) Spielman, L. A. *The scientific basis of flocculation*; Ives, K. J., Ed.; Sijthoff and Noordhoff: Alphen aan den Rijn, The Netherlands, 1978; pp 63–99.
- (38) Parker, D. S.; Kaufman, W. J.; Jenkins, D. *J. San. Eng. Div., Proc. Am. Soc. Civil Eng.* **1972**, *98* (SA1), 79–99.
- (39) Pandya, J. D.; Spielman, L. A. *J. Colloid Interface Sci.* **1982**, *90*, 517–531.
- (40) Hill, P. S. *Deep-Sea Res.* **1996**, *43*, 679–702.
- (41) Jackson, G. A. *Deep-Sea Res. II* **1995**, *42*, 215–222.
- (42) Allredge, A. L.; Granata, T. C.; Gotschalk, C. C.; Dickey, T. D. *Limnol. Oceanogr.* **1990**, *35*, 1415–1428.
- (43) Jackson, G. A. *Deep-Sea Res. II* **1995**, *42*, 159–184.
- (44) Al Ani, S.; Dyer, K. R.; Huntley, D. A. *Geo-Mar. Lett.* **1991**, *11*, 154–158.
- (45) Müller-Niklas, G.; Schuster, S.; Kaltenböck, E.; Herndl, G. J. *Limnol. Oceanogr.* **1994**, *39*, 58–68.
- (46) Smith, D. C.; Steward, G. F.; Long, R. F.; Azam, F. *Deep-Sea Res. II* **1995**, *42*, 75–97.
- (47) Buffle, J.; Leppard, G. G. *Environ. Sci. Technol.* **1995**, *29*, 2169–2175.
- (48) Buffle, J.; Leppard, G. G. *Environ. Sci. Technol.* **1995**, *29*, 2176–2184.
- (49) Buffle, J.; Perret, D.; Newman, M. *Environmental Particles*, Vol. 1; Buffle, J., van Leeuwen, H. P., Eds.; Lewis Publishers: Chelsea, MI, 1993; pp 171–230.
- (50) Jiang, Q.; Logan, B. E. *J. Am. Water Works Assoc.* **1996**, *88*, 100–113.
- (51) Simpson, W. R. *Oceanogr. Mar. Biol. Annu. Rev.* **1991**, *20*, 119–172.
- (52) Koike, I. S.; Hara, S.; Terauchi, T.; Kogure, K. *Nature* **1990**, *345*, 242–244.
- (53) Wells, M. L.; Goldberg, E. D. *Nature* **1991**, *353*, 467–469.
- (54) Wells, M. L.; Goldberg, E. D. *Mar. Chem.* **1992**, *40*, 5–18.
- (55) Wells, M. L.; Goldberg, E. D. *Mar. Chem.* **1993**, *41*, 353–358.
- (56) Wells, M. L.; Goldberg, E. D. *Limnol. Oceanogr.* **1994**, *39*, 286–302.
- (57) Sheldon, R. W.; Prakash, A.; Sutcliffe, W. H. *Limnol. Oceanogr.* **1972**, *17*, 327–340.
- (58) Sheldon, R. W.; Prakash, A.; Sutcliffe, W. H. *Limnol. Oceanogr.* **1973**, *18*, 719–733.
- (59) Lal, D.; Lerman, A. *J. Geophys. Res.* **1975**, *80*, 423–430.
- (60) Lerman, A.; Carder, K. L.; Betzer, P. R. *Earth Planet. Sci. Lett.* **1977**, *37*, 61–70.
- (61) McCave, I. N. *Deep-Sea Res.* **1975**, *22*, 491–502.
- (62) McCave, I. N. *Deep-Sea Res.* **1984**, *31*, 329–352.
- (63) Bishop, J. K. B.; Ketten, D. R.; Edmond, J. M. *Deep-Sea Res.* **1978**, *25A*, 1121–1161.
- (64) Bishop, J. K. B.; Collier, R. W.; Kitten, D. R.; Edmond, J. M. *Deep-Sea Res.* **1980**, *27*, 615–640.
- (65) Suzuki, N.; Kato, K. *Bull. Faculty Fish Hokkaido Univ.* **1953**, *4*, 132–135.
- (66) Silver, M. W.; Shanks, A. L.; Trent, J. D. *Science* **1978**, *201*, 371–373.
- (67) Allredge, A. L.; Silver, M. W. *Prog. Oceanogr.* **1988**, *20*, 41–82.
- (68) Kranck, K.; Milligan, T. G. *Mar. Ecol. Prog. Ser.* **1988**, *44*, 183–189.
- (69) Asper, V. L. *Deep-Sea Res.* **1987**, *34*, 1–17.
- (70) Silver, M. W.; Gowing, M. M. *Prog. Oceanogr.* **1991**, *26*, 75–113.
- (71) Lampitt, R. S.; Hillier, W. R.; Challenor, P. G. *Nature* **1993**, *362*, 737–739.
- (72) Deuser, W. G.; Ross, E. H.; Anderson, R. F. *Deep-Sea Res.* **1981**, *28A*, 495–505.
- (73) Asper, V. L.; Deuser, W. G.; Knauer, G. A.; Lohrenz, S. E. *Nature* **1992**, *357*, 670–672.
- (74) Lampitt, R. S.; Wishner, K. F.; Turley, C. M.; Angel, M. V. *Mar. Biol.* **1993**, *116*, 689–702.
- (75) Ruiz, J. *Deep-Sea Res.* **1997**, *44*, 1105–1126.
- (76) Graham, W. M. University of California, Santa Barbara, 1998, Personal communication.
- (77) Walsh, I. D.; Gardner, W. D. *Deep-Sea Res.* **1992**, *39*, 1817–1834.
- (78) Miquel, J. C.; Fowler, S. W.; La Rosa, J.; Buat-Menard, P. *Deep-Sea Res.* **1994**, *41*, 243–261.
- (79) Marty, J. C.; Nicolas, E.; Miquel, J. C.; Fowler, S. W. *Mar. Chem.* **1994**, *46*, 387–405.
- (80) Newton, P. P.; Lampitt, R. S.; Jickells, T. D.; King, P.; Boutle, C. *Deep-Sea Res. I* **1994**, *41*, 1617–1642.
- (81) Billet, D. S. M.; Lampitt, R. S.; Rice, A. L.; Mantoura, R. F. C. *Nature* **1983**, *302*, 520–522.

- (82) Lochte K.; Turley, C. M. *Nature* **1988**, 333, 67–69.
- (83) Thiel, H.; Pfannkuche, O.; Schriever, G.; Lochte, K.; Gooday, A. J.; Hemleben, V.; Mantoura, R. F. G.; Turley, C. M.; Patching, J. W.; Riemann, F. *Biol. Oceanogr.* **1990**, 6, 203–239.
- (84) Alldredge, A. L.; Passow, U.; Logan, B. E. *Deep-Sea Res.* **1993**, 40, 1131–1140.
- (85) Passow, U.; Logan, B. E.; Alldredge, A. L. *Deep-Sea Res.* **1994**, 41, 335–357.
- (86) Mari, X.; Kjørboe, T. *J. Plankton Res.* **1996**, 18, 969–986.
- (87) Kjørboe, T.; Hansen, J. L. S. *J. Plankton Res.* **1993**, 15, 993–108.
- (88) Passow, U.; Wassmann, P. *Mar. Ecol.-Prog. Ser.* **1994**, 104, 153–161.
- (89) Mopper, K.; Zhou, J.; Sri Ramana, K.; Passow, U.; Dam, H. G.; Drapeau, D. T. *Deep-Sea Res. II* **1995**, 42, 47–73.
- (90) Passow, U.; Alldredge, A. L. *Deep-Sea Res. II* **1995**, 42, 99–109.
- (91) Logan, B. E.; Passow, U.; Alldredge, A. L.; Grossart, H. P.; Simon, M. *Deep-Sea Res. II* **1995**, 42, 203–214.
- (92) Crocker, K. M.; Passow, U. *Mar. Ecol. Prog. Ser.* **1995**, 117, 249–257.
- (93) Kjørboe, T.; Tiselius, P.; Mitchell-Innes, B.; Hansen, J. L. S.; Visser, A. W.; Mari, X. *Limnol. Oceanogr.* **1998**, 43, 104–116.
- (94) Kjørboe, T.; Lundsgaard, C.; Olesen, M.; Hansen, J. *J. Mar. Res.* **1994**, 52, 297–323.
- (95) Platt, T.; Denman, K. *Helgol. Wiss. Meeresunters.* **1977**, 30, 575–581.
- (96) Platt, T.; Denman, K. *Rapp. P.-V. Reun. Cons. Int. Explor. Mer* **1978**, 173, 60–65.
- (97) Rodriguez, J.; Mullin, M. M. *Ecology* **1986**, 67, 215–222.
- (98) Jiang, Q.; Logan, B. E. *Environ. Sci. Technol.* **1991**, 25, 2031–2038.
- (99) Burd, A. B.; Jackson, G. A. 1998, Personal communication.
- (100) Farley, K.; Morel, F. M. M. *Environ. Sci. Technol.* **1986**, 20, 187–195.
- (101) Burd, A.; Jackson, G. A. *J. Geophys. Res.* **1997**, 102, 10,545–10,561.
- (102) Barrett, J. C.; Webb, N. A. *J. Aerosol Sci.* **1998**, 29, 31–39.
- (103) Gelbard, F.; Tambour, Y.; Seinfeld, J. H. *J. Colloid Interface Sci.* **1980**, 76, 541–556.
- (104) Jackson, G. A.; Lochmann, S. E. *Limnol. Oceanogr.* **1992**, 37, 77–89.
- (105) Hahn, H. H.; Stumm, W. *Am. J. Sci.* **1970**, 268, 354–368.
- (106) Sholkovitz, E. R. *Geochim. Cosmochim. Acta* **1976**, 40, 831–845.
- (107) Sholkovitz, E. R.; Copland, D. *Geochim. Cosmochim. Acta* **1981**, 45, 181–189.
- (108) Kranck, K.; Milligan T. G. *J. Geophys. Res.* **1992**, 97, 11,373–11,382.
- (109) Jackson, G. A. *Deep-Sea Res.* **1990**, 37, 1197–1211.
- (110) Riebesell, U. *Mar. Ecol. Prog. Ser.* **1991**, 69, 281–291.
- (111) Kjørboe, T.; Andersen, K. P.; Dam, H. G. *Mar. Biol.* **1990**, 107, 235–245.
- (112) Hill, P. S. *J. Geophys. Res.* **1992**, 9, 2295–2308.
- (113) Mari, X.; Burd, A. *Mar. Ecol. Prog. Ser.* **1998**, 163, 63–76.
- (114) Stoll, S.; Buffle, J. *J. Colloid Interface Sci.* **1996**, 180, 548–563.
- (115) Kjørboe, T.; Hansen, J. L. S.; Alldredge, A. L.; Jackson, G. A.; Passow, U.; Dam, H. G.; Drapeau, D. T.; Waite, A.; Garcia, C. *J. Mar. Res.* **1996**, 54, 1123–1148.
- (116) Buesseler, K. O.; Bacon, M. P.; Cochran, J. K.; Livingston, H. D. *Deep-Sea Res.* **1992**, 39, 1115–1137.
- (117) Cochran, J. K.; Buesseler, K. O.; Bacon, M. P.; Livingston, H. D. *Deep-Sea Res.* **1993**, 40, 1569–1595.
- (118) Buesseler, K. O.; Andrews, A. D.; Hartman, M. C.; Belastock, R.; Chai, F. *Deep-Sea Res. II* **1995**, 42, 777–804.
- (119) Bacon, M. P.; Cochran, J. K.; Hirschberg, D.; Hammer, T. R.; Fleer, A. P. *Deep-Sea Res. II* **1996**, 43, 1133–1153.
- (120) Murray, J. W.; Young, J.; Newton, J.; Dunne, J.; Chapin, T.; Paul, B.; McCarthy, J. J. *Deep-Sea Res. II* **1996**, 43, 1095–1132.
- (121) Moran, S. B.; Ellis, K. M.; Smith, J. N. *Deep-Sea Res. II* **1997**, 44, 1593–1606.
- (122) Honeyman, B. D.; Santschi, P. H. *J. Mar. Res.* **1989**, 47, 951–992.
- (123) Clegg, S. L.; Whitfield, M. *Deep-Sea Res.* **1993**, 40, 1529–1545.
- (124) Moran, S. B.; Buesseler, K. O. *Nature* **1993**, 359, 221–223.
- (125) Burd, A.; Moran, S. B.; Jackson, G. A. A coupled adsorption-aggregation model of the POC/²³⁴Th ratio of marine particles. *Deep Sea Res.* Submitted for publication.
- (126) Niven, S. E. H.; Kepkay, P. E.; Boraie, A. *Deep-Sea Res. II* **1995**, 42, 257–273.
- (127) Murname, R. J.; Cochran, J. K.; Buesseler, K. O.; Bacon, M. P. *Deep-Sea Res.* **1996**, 43, 239–258.
- (128) Baskaran, M.; Santschi, P. H.; Benoit, G.; Honeyman, B. D. *Geochim. Cosmochim. Acta* **1992**, 56, 3375–3388.

Received for review March 16, 1998. Revised manuscript received June 1, 1998. Accepted June 15, 1998.

ES980251W